Topographic Modeling of Free and Methionyl-tRNA Synthetase Bound $tRNA^{fMet}$ by Singlet-Singlet Energy Transfer: Bending of the 3'-Terminal Arm in $tRNA^{fMet}$†

Blair Q. Ferguson‡ and David C. H. Yang*
Department of Chemistry, Georgetown University, Washington, D.C. 20057
Received April 2, 1986; Revised Manuscript Received June 30, 1986

ABSTRACT: Conformations of $tRNA^{fMet}$, free and methionyl-tRNA synthetase bound forms, are analyzed by using singlet-singlet energy transfer as a spectroscopic ruler. $tRNA^{fMet}$(8-13,3'-Flc), $tRNA^{fMet}$(8-13,D-Etd), and $tRNA^{fMet}$(3'-Flc,D-Etd) are prepared by sequential chemical modifications. The methionyl-tRNA synthetase binding affinity of these double-labeled $tRNA^{fMet}$s is similar to those of unmodified $tRNA^{fMet}$. The fluorescence properties of the individual fluorophore in these tRNAs, including emission spectra, anisotropy, and quenching by methionyl-tRNA synthetase, are similar to those of single-labeled $tRNA^{fMet}$. The transfer efficiencies of double-labeled $tRNA^{fMet}$s, as determined by both donor quenching and sensitized emission, showed efficient energy transfer in all cases. Random orientation being assumed, the apparent distances are 25 Å between 8-13 and D20, 44 Å between 8-13 and the 3'-terminus, and 49 Å between the 3'-terminus and D20, respectively, in free $tRNA^{fMet}$. Upon binding of methionyl-tRNA synthetase, the apparent distances are 25 Å between 8-13 and D20, 45 Å between 8-13 and the 3'-terminus, and 54 Å between the 3'-terminus and D20, respectively. These results provide topographic models of these specific locations in free and methionyl-tRNA synthetase bound $tRNA^{fMet}$ and suggest that the immobilized 3'-terminal arm in the amino acid acceptor stem bends toward the inner loop of the L-shaped tRNA upon binding of methionyl-tRNA synthetase.

Nucleic acid-protein recognition has been extensively studied. It has become increasingly clear that conformational changes in both the nucleic acids and the proteins play critical roles in the mutual adaptation processes. Interaction of $tRNA^{fMet}$ and methionyl-tRNA synthetase has been used as one of the model systems in the elucidation of the general characteristics of RNA-protein recognition (Schimmel & Soll, 1979). The high-resolution crystal structures of both $tRNA^{fMet}$ (Woo et al., 1980) and an active fragment (Cassio & Waller, 1974) of methionyl-tRNA synthetase (Zelwer et al., 1982) have been determined. Extensive studies of their interaction have been carried out by a variety of approaches, including photo-cross-linking (Ackerman et al., 1985; Rosa et al., 1979), chemical modification (Schulman et al., 1983), base substitution (Uemura et al., 1982), fluorescence spectroscopy (Blanquet et al., 1973; Ferguson & Yang, 1986a), neutron scattering (Dessen et al., 1982), and affinity chemical modification (Wetzel & Soll, 1977; Hountondji et al., 1985). All evidence appears to be consistent with the general picture that the synthetase binds the inner loop of the L-shaped tRNA molecules.

Relatively little is known as to the conformation of synthetase-bound tRNA. In a comparison of fluorescence properties of the fluorescent-labeled $tRNA^{fMet}$ with those of enzyme-bound $tRNA^{fMet}$, 3'-terminal and delocalized conformational changes were found, on the basis of changes in the local environment, anisotropy, and solvent accessibility (Ferguson & Yang, 1986a). To further define the conformation of tRNA and the tRNA-synthetase complex, we analyzed the proximity relationship among different locations in $tRNA^{fMet}$ using singlet-singlet energy transfer.

Singlet-singlet energy transfer of fluorescent-labeled tRNA has been previously applied to the conformational studies of tRNA in solution (Beardsley & Cantor, 1970; Yang & Soll, 1973) and the tRNA-ribosome complexes (Fairclough & Cantor, 1979; Wells & Cantor, 1980). Since the efficiency of energy transfer depends on the proximity as well as the relative orientation of the donor and the acceptor (Forster, 1966; Cantor & Schimmel, 1980), energy transfer provides a highly sensitive method for the detection of conformational changes of macromolecules. In addition, conformational constraints in terms of the apparent distances can be derived from the observed transfer efficiency.

In this paper, we report the results of the conformational analysis of free and MetRS[1]-bound $tRNA^{fMet}$ using $tRNA^{fMet}$ bearing two fluorescent groups. Topographic models of tRNA are constructed on the basis of the present results.

Materials and Methods

Aminoacylation assay and fluorescence measurements including fluorescence titration, anisotropy, and dynamic quenching were carried out as previously described (Ferguson & Yang, 1986a). Preparation and characterization of MetRS and fluorescent-labeled $tRNA^{fMet}$, including $tRNA^{fMet}$(3'-Flc), $tRNA^{fMet}$(8-13), and $tRNA^{fMet}$(D-Etd) have been described (Ferguson & Yang, 1986a). Titrations of MetRS and

† This work was supported by grants from NIH (GM-25848) and NSF (81-10818).
* Author to whom correspondence should be addressed.
‡ Present address: Du Pont Experimental Station, Wilmington, DE 19898.

[1] Abbreviations: Flc, fluorescein; Etd, ethidium; MetRS, methionyl-tRNA synthetase; $tRNA^{fMet}$(8-13,D-Etd), $tRNA^{fMet}$ with reduced, photo-cross-linked S8-C13 and ethidium replacing D20; $tRNA^{fMet}$(8-13,3'-Flc), $tRNA^{fMet}$ with fluorescein thiosemicarbazide at 3'-terminus and reduced photo-cross-linked S8-C13; $tRNA^{fMet}$(3'-Flc,D-Etd), $tRNA^{fMet}$ with D20 replaced with ethidium and fluorescein thiosemicarbazide at 3'-terminus.

0006-2960/86/0425-6572$01.50/0

fluorescent-labeled tRNA were carried out and analyzed as previously described (Ferguson & Yang, 1986a).

Preparation of tRNA^{fMet}(8–13,3′-Flc). tRNA^{fMet}(8–13) was labeled at the 3′-terminus with Flc under the same conditions described for the preparation of tRNA^{fMet}(3′-Flc) (Wells & Cantor, 1977; Ferguson & Yang, 1986a). Treatment of tRNA^{fMet}(8–13) with periodate reduced the 8–13 emission intensity by 10%. The stoichiometry of labeling of tRNA^{fMet}(8–13,3′-Flc) was determined from the absorption spectrum of purified tRNA^{fMet}(8–13,3′-Flc). The absorbance of the 3′-Flc and 8–13 fluorophores was corrected for the contribution of 8–13 and 3′-Flc, respectively, by reference to the absorption spectra of the corresponding single-labeled tRNA^{fMet}s.

Preparation of tRNA^{fMet}(8–13,D-Etd). tRNA^{fMet} was photo-cross-linked as described previously (Favre et al., 1971; Ferguson & Yang, 1986a). The same conditions are used for $NaBH_4$ reduction of the s^4U8–C13 photo-cross-link and the D20 nucleotide. Following $NaBH_4$ reduction, the D20 nucleotide was replaced with Etd by the procedure described for the preparation of tRNA^{fMet}(D-Etd) (Wintermeyer & Zachau, 1979). The stoichiometry of labeling of tRNA^{fMet}(8–13,D-Etd) was determined from the absorption spectrum of tRNA^{fMet}(8–13,D-Etd). The D-Etd and 8–13 absorbance was corrected for the contribution of 8–13 and D-Etd absorbance, respectively, by reference to absorption spectra for the corresponding single-labeled tRNA^{fMet}s.

Preparation of tRNA^{fMet}(3′-Flc,D-Etd). tRNA^{fMet}(D-Etd) was periodate-oxidized and reacted with Flc under the same conditions described for the preparation of tRNA^{fMet}(3′-Flc). Periodate oxidation did not alter the emission intensity of tRNA^{fMet}(D-Etd). The 3′-Flc labeling stoichiometry was determined from the absorption spectrum of tRNA^{fMet}(3′-Flc,D-Etd). The 3′-Flc absorbance was corrected for the contribution of D-Etd by reference to the absorption spectrum of tRNA^{fMet}(D-Etd). The labeling stoichiometry was determined by comparing the D-Etd emission intensity at 600 nm (λ_{ex} = 320 nm) in tRNA^{fMet}(3′-Flc,D-Etd) and tRNA^{fMet}(D-Etd).

Measurement of Energy-Transfer Efficiency. The apparent transfer efficiency (E_D) was measured as the extent of quenching of the donor emission with eq 1 (Fairclough & Cantor, 1978), where $F^D_{DA}(\lambda^{ex}_D,\lambda^{em}_D)$ and $F^D_D(\lambda^{ex}_D,\lambda^{em}_D)$ are the emission intensity of donor in the presence and in the absence of the acceptor with the excitation wavelength (λ^{ex}_D) and the emission wavelength (λ^{em}_D) of the donor. The excitation and emission spectra of the donors are not shifted in the presence of the acceptor in the present cases. Inner filter effect and dilution are corrected.

$$E_D = 1 - F^D_{DA}(\lambda^{ex}_D,\lambda^{em}_D)/F^D_D(\lambda^{ex}_D,\lambda^{em}_D) \quad (1)$$

The apparent transfer efficiency was also determined from the sensitized emission with eq 2 (Fairclough & Cantor, 1978), where $A^A_{DA}(\lambda_D)$ and $A^D_{DA}(\lambda_D)$ are the absorbances of the acceptor and the donor at the donor's absorption wavelength of the sample with both donor and acceptor and $F^A_{DA}(\lambda^{ex}_D,\lambda^{em}_A)$ and $F^D_A(\lambda^{ex}_D,\lambda^{em}_A)$ are the emission intensity of the acceptor in the presence (sensitized emission) or absence of the donor at the emission wavelength of the acceptor and the excitation wavelength of the donor. The intensity of the sensitized emission was corrected for the contribution of donor emission with species containing donor only. The absorbance of the donor or acceptor was determined from the respective extinction coefficient, the molar concentration of tRNA^{fMet}, and the labeling stoichiometry. For a given energy-transfer experiment, all measurements for different samples are carried out at the same time with identical instrumental settings to minimize necessary corrections.

$$E_A = \frac{A^A_{DA}(\lambda_D)}{A^D_{DA}(\lambda_D)}\left[\frac{F^A_{DA}(\lambda^{ex}_D,\lambda^{em}_A)}{F^D_A(\lambda^{ex}_D,\lambda^{em}_A)} - 1\right] \quad (2)$$

The apparent transfer efficiency from eq 1 or 2 was corrected for the acceptor binding stoichiometry with eq 3, where

$$E_{cor} = E_{app}/f_A \quad (3)$$

E_{app}, E_{cor}, and f_A are the apparent transfer efficiency (E_A or E_D), the corrected transfer efficiency, and the fraction of tRNA^{fMet} containing acceptor molecules.

Calculation of Apparent Distances. The relation of the transfer efficiency of singlet–singlet energy transfer and the proximity between donor and acceptor has been shown (Forster, 1966) as

$$R = (1/E - 1)^{1/6}R_0 \quad (4)$$

where $R_0 = [(8.79 \times 10^{-5})K^2n^{-1}\phi_D J_{DA}]^{1/6}$ and R and E are the apparent distance and the transfer efficiency. The overlap integral, J, was computed by numerical integration. The refractive index, n, was taken as 1.4 (Fairclough & Cantor, 1978). Quantum yield of the donor, ϕ_D, was determined from the relative quantum yield and corrected emission spectra and was corrected for the polarization effect (Shinisky, 1972).

The orientation factor, K^2, was treated according to Hass et al. (1978). The anisotropy of the fluorophores in fluorescent-labeled tRNA^{fMet} has been previously determined (Ferguson & Yang, 1986a).

Results

tRNA^{fMet}(8–13,D-Etd). tRNA^{fMet}(8–13,D-Etd) was prepared as described in under Materials and Methods. tRNA^{fMet}(8–13,D-Etd) contains 0.97 mol of 8–13 and 0.90 mol of D-Etd per mole of tRNA^{fMet}.

The properties of tRNA^{fMet}(8–13,D-Etd) are compared with the single-labeled tRNA^{fMet}(8–13) and tRNA^{fMet}(D-Etd) as shown in Table I. The absorption, excitation, and emission maximum wavelengths of the 8–13 and D-Etd fluorophores in tRNA^{fMet}(8–13,D-Etd) are the same as those for the corresponding single-labeled tRNA^{fMet}. In addition, the steady-state anisotropy and the limiting anisotropy and the slope of the Perrin plot for the fluorophores in tRNA^{fMet}(8–13,D-Etd) are close to those of the corresponding single-labeled tRNA^{fMet}. These results indicate that the structure and the local environment of the fluorophore are not significantly perturbed by the additional modification.

As shown in Table I, tRNA^{fMet}(8–13,D-Etd) can be aminoacylated with methionine by MetRS to an extent of about 70% of that for unmodified tRNA^{fMet}. The acceptor activity of tRNA^{fMet}(8–13,D-Etd) was greater than that of tRNA^{fMet}(D-Etd). The MetRS binding constant and the extent of MetRS tryptophan quenching for tRNA^{fMet}(8–13,D-Etd) are close to those of the corresponding single-labeled tRNA^{fMet}, which are, in turn, very similar to the values for unmodified tRNA^{fMet}. Upon binding of MetRS, tRNA^{fMet}(8–13,D-Etd) exhibited the emission anisotropy and excitation and emission maximum wavelengths similar to those of the corresponding MetRS-bound single-labeled tRNA^{fMet}. The MetRS-induced quenching in D-Etd emission intensity is similar for tRNA^{fMet}(D-Etd) and tRNA^{fMet}(8–13,D-Etd) (Table I). These results suggest that the interaction of the double-labeled tRNA^{fMet}(8–13,D-Etd) with MetRS is very similar to that for single-labeled tRNA^{fMet}(8–13) and

Table I: Properties of Fluorescent Single-Labeled and Double-Labeled $tRNA^{fMet}$s, Free and in Complex with MetRS

modified $tRNA^{fMet}$	fluorophore	labeling stoichiometry (mol of $tRNA^{fMet}$)	acceptor act. (nmol/A_{260})	MetRS binding parameters (Trp quenching): dissociation constant, K (μM)	$(F/F_0)_{max}$	excitation wavelength maximum, λ_{max}^{ex} (nm)	emission wavelength maximum, λ_{max}^{em} (nm)[b]	anisotropy, r	limiting anisotropy, r_0[d]	emission intensity relative to free tRNA, $(F/F_0)_{max}$[e]	dissociation constant, K (μM)[e]
$tRNA^{fMet}$ (8–13)	8–13	0.92	1.5	0.46	0.52	388 (388)[a]	436 (436)[a]	0.256 (0.287)[a]	0.305	1.00	nd
$tRNA^{fMet}$ (D-Etd)	D-Etd	0.80	0.70	0.40	0.55	515 (513)	595 (598)	0.196 (0.250)	0.287	0.96	nd
$tRNA^{fMet}$ (3′-Flc)	3′-Flc	0.98	0.0	0.14	0.42	493 (498)	518 (523)	0.062 (0.197)	0.204	0.58	0.10
$tRNA^{fMet}$ (8–13, D-Etd)	8–13	0.97	1.1	0.45	0.55	388 (388)	436 (436)	0.258 (0.286)	0.299	1.04	nd
$tRNA^{fMet}$ (8–13, D-Etd)	D-Etd	0.90				515 (513)	595 (598)	0.203 (0.248)	0.282	0.96	nd
$tRNA^{fMet}$ (8–13, 3′-Flc)	8–13	0.92	0.0	0.15	0.41	388 (388)	436 (436)	0.252 (0.283)	0.305	1.06	nd
$tRNA^{fMet}$ (8–13, 3′-Flc)	3′-Flc	0.98				493 (498)	518 (523)	0.063 (0.190)	0.204	0.59	0.13
$tRNA^{fMet}$ (3′-Flc, D-Etd)	3′-Flc	0.92	0.0	0.50	0.60	493 (496)	518 (523)	0.060 (0.180)	0.204	0.65	0.15
$tRNA^{fMet}$ (3′-Flc, D-Etd)	D-Etd[f]	0.75				nd	nd	nd	nd	nd	nd

[a] Numbers in parentheses are values for the tRNA–synthetase complex. [b] Values are determined from spectra that have not been corrected for the wavelength dependence of the fluorometer detection system sensitivity. [c] Determined in standard buffer at 20 °C. [d] Determined from the intercept of a Perrin plot; according to eq 3 in Ferguson and Yang (1986a). [e] Determined by fitting data, obtained by the titration of tRNA with MetRS, according to eq 2 in Ferguson and Yang (1986a), where $n = 1.0$. [f] The fluorescence properties of the D-Etd fluorophore in $tRNA^{fMet}$ (3′-Flc,D-Etd) could not be determined with precision due to the very strong overlapping contribution of 3′-Flc emission.

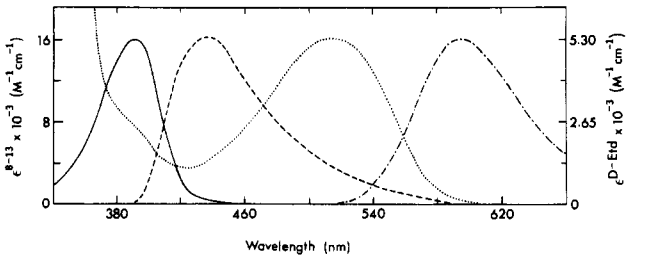

FIGURE 1: Spectra of the 8–13 donor and the D-Etd acceptor in $tRNA^{fMet}$(8–13,D-Etd). The excitation (—) and corrected emission (– –) spectra in $tRNA^{fMet}$(8–13) are shown. Also shown are the D-Etd absorption (···) and emission (–·–) spectra for $tRNA^{fMet}$(D-Etd).

Table II: Energy-Transfer Parameters for Free and MetRS-Bound $tRNA^{fMet}$(8–13,D-Etd)

parameter[a]	free $tRNA^{fMet}$-(8–13,D-Etd)	MetRS-bound $tRNA^{fMet}$-(8–13,D-Etd)
donor	8–13	8–13
acceptor	D-Etd	D-Etd
J (M^{-1} cm^{-1} nm^4)	1.3×10^{14}	1.3×10^{14}
ϕ_D	0.60	0.60
$R_0(2/3)$ (Å)	33	33
E_D	0.77	0.76
E_A	0.76	nd
f_A (mol of acceptor/mol of $tRNA^{fMet}$)	0.90	0.90
E_D^{cor}	0.86	0.84
$R(2/3)$ (Å)	25	25
$R(2/3)/R$	0.89–1.13	0.89–1.13
R (Å)	22–28	22–28

[a] The parameters are defined under Materials and Methods: J, spectral overlap; ϕ_D, quantum yield of donor; $R_0(2/3)$, characteristic distance with $K^2 = 2/3$; E_D, transfer efficiency by donor quenching; E_A, transfer efficiency by sensitized emissions; f_A, fractional occupancy of Etd; E_D^{cor}, corrected transfer efficiency; $R(2/3)$, apparent distance separating the donor and the acceptor with $R_0(2/3)$; $R(2/3)/R$, range of ratios of distances with a probability parameter (Q) of 0.5 and the apparent distance based on the anisotropy of the fluorophores according to Haas et al (1978); R, range of distances with a probability parameter (Q) of 0.5.

$tRNA^{fMet}$(D-Etd) and in turn to that of unmodified $tRNA^{fMet}$.

The spectral overlap integral for the 8–13 donor and D-Etd acceptor was calculated with the corrected emission spectrum for $tRNA^{fMet}$(8–13) and the absorption spectrum for $tRNA^{fMet}$(D-Etd). These spectra are shown in Figure 1. $R_0(2/3)$ for the 8–13 donor and D-Etd acceptor was calculated to be 33 Å (Table II).

The energy-transfer efficiency between the 8–13 and D-Etd in $tRNA^{fMet}$(8–13,D-Etd) was determined by measuring both the donor quenching (E_D) and the sensitized emission (E_A). Donor quenching, F_{DA}^{D}, was monitored at 440 nm (λ_{ex} = 390 nm), and sensitized emission, F_{DA}^{A}, was monitored at 600 nm (λ_{ex} = 390 nm). The emission intensities, F_D^D and F_A^D, were determined from the fluorescence spectra for $tRNA^{fMet}$(8–13) and $tRNA^{fMet}$(D-Etd), respectively. The energy-transfer parameters for $tRNA^{fMet}$(8–13,D-Etd) are summarized in Table II. The transfer efficiency measured by donor quenching is in close agreement with that by sensitized emission, suggesting that Forster energy transfer accounts for the 8–13 quenching. In practice, the transfer efficiency can be measured with greater precision by donor quenching than by sensitized acceptor emission. This is due to the nature of the defining equations and because the 8–13 emission intensity is much greater than the D-Etd emission intensity. Having established that the donor quenching is due to Forster energy transfer, the transfer efficiency in the presence of MetRS was determined by measuring donor quenching only.

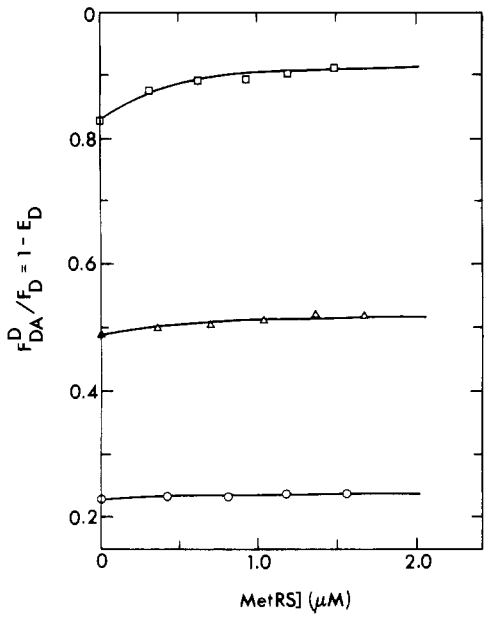

FIGURE 2: Fluorescence titration of 0.91 μM tRNA^{fMet}(8–13,D-Etd) (○), 0.37 μM tRNA^{fMet}(8–13,3′-Flc) (△), and 0.41 μM tRNA^{fMet}-(3′-Flc,D-Etd) (□) with MetRS, as monitored by the change in energy-transfer efficiency. The energy-transfer efficiency, E_D, was determined by measuring the extent of donor quenching. The emission intensity of the donor emission intensity occurs in the absence of the acceptor. The quantities F^D_{DA} and F_D are defined in the text. The solid curves have been calculated with eq 2 in Ferguson & Yang (1986a). The binding parameters [K (μM), $\Delta(1 - E_D)_{max}$, and n, respectively] used to fit the data are as follows: tRNA^{fMet}(8–13,D-Etd), 0.12, 0.015, 1.0; tRNA^{fMet}(8–13,3′-Flc), 0.14, 0.033, 1.0; tRNA^{fMet}(3′-Flc,D-Etd), 0.12, 0.090, 1.0.

tRNA^{fMet}(8–13,D-Etd) was titrated with MetRS, and the emission intensity of the 8–13 donor was monitored. The change in $1 - E_D$ with increasing concentration of MetRS is shown in Figure 2. The overlap integral is identical for free and MetRS-bound tRNA^{fMet}(8–13,D-Etd) (Table II). The quantum yield of tRNA^{fMet}(8–13) is not changed when the tRNA is complexed with MetRS (Ferguson & Yang, 1986a). $R_0(2/3)$ is, therefore, expected to be identical for free and MetRS-bound tRNA^{fMet}(8–13,D-Etd). Given the above considerations, it is apparent that any change in the donor emission in tRNA^{fMet}(8–13,D-Etd) intensity on binding to MetRS reflects a change in the energy-transfer efficiency. The energy-transfer parameters for tRNA^{fMet}(8–13,D-Etd), in complex with MetRS, are given in Table II.

The energy-transfer efficiency for the 8–13 donor and D-Etd acceptor in free tRNA^{fMet}(8–13,D-Etd) is determined to be 0.86 (Table II). The distance separating the 8–13 and D-Etd positions in free tRNA^{fMet}(8–13,D-Etd) is calculated to be 25 ± 3 Å. Addition of MetRS to tRNA^{fMet}(8–13,D-Etd) induces a small increase in the 8–13 emission intensity that corresponds to a reduced transfer efficiency (0.84). The maximal MetRS-induced increase in donor emission intensity, when all tRNA^{fMet}(8–13,D-Etd) is bound to MetRS, was calculated from the data and the fitting binding function given in Figure 2. The calculated apparent distance separating the 8–13 and D-Etd fluorophores in MetRS-bound tRNA^{fMet}(8–13,D-Etd) is 25 ± 3 Å. These results suggest that the apparent distance and orientation between the 8–13 and D-Etd probes are virtually unchanged when tRNA^{fMet}(8–13,D-Etd) complexes with MetRS. Upon binding of MetRS, there is an increase in the emission anisotropy of 8–13 and D-Etd in tRNA^{fMet}(8–13,D-Etd) (Table I). In the present case, the relatively small increase in acceptor and donor anisotropy does not affect the range of the apparent distance "R" due to the uncertainty in the orientation factor (Haas et al., 1978).

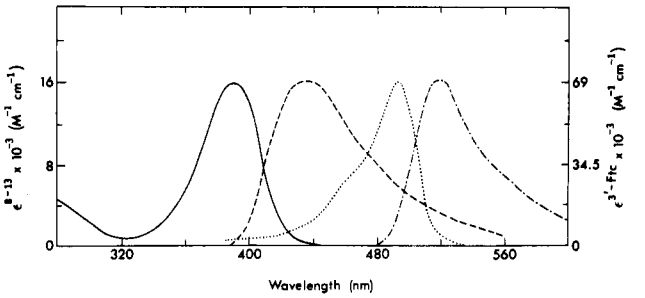

FIGURE 3: Spectral relationships characterizing the 8–13 donor and the 3′-Flc acceptor in tRNA^{fMet}(8–13,3′-Flc). The 8–13 excitation (—) and corrected emission (– –) spectra in tRNA^{fMet}(8–13) are shown. Also shown are the 3′-Flc absorption (···) and corrected emission (–·–) spectra for tRNA^{fMet}(3′-Flc).

tRNA^{fMet}(8–13,3′-Flc). tRNA^{fMet}(8–13,3′-Flc) was prepared as described under Materials and Methods. tRNA^{fMet}(8–13,3′-Flc) contains 0.92 mol of 8–13 and 0.98 mol of Flc per mole of tRNA^{fMet}.

The properties of tRNA^{fMet}(8–13,3′-Flc) are compared with the single-labeled tRNA^{fMet}(8–13) and tRNA^{fMet}(3′-Flc) as shown in Table I. Periodate oxidation of tRNA^{fMet}(8–13) results in a 10% loss of the 8–13 emission. The absorption, excitation, and emission maximum wavelengths as well as the steady-state anisotropy and Perrin plot's limiting anisotropy and slope of the fluorophores are the same for tRNA^{fMet}(8–13,3′-Flc) and the corresponding single-labeled tRNA^{fMet}s.

Following 3′-labeling, tRNA^{fMet} cannot be aminoacylated with methionine by MetRS. However, 3′-fluorescein-labeled tRNA^{fMet} does bind to MetRS with the same affinity and induces close to the same extent of MetRS tryptophan quenching as unmodified tRNA^{fMet} (Ferguson & Yang, 1986a). The MetRS binding affinity and extent of tryptophan quenching for the double-labeled tRNA^{fMet}(8–13,3′-Flc) are similar to the values determined for the corresponding single-labeled tRNA^{fMet}s (Table I). The binding constant determined from the quenching of 3′-Flc emission by MetRS and the maximal extent of 3′-Flc quenching induced by MetRS are very similar for tRNA^{fMet}(8–13,3′-Flc) and tRNA^{fMet}-(3′-Flc) (Table I).

The overlap integral for the 8–13 donor and 3′-Flc acceptor was calculated with the corrected emission spectrum of tRNA^{fMet}(8–13) and the absorption spectrum of tRNA^{fMet}-(3′-Flc) (Figure 3). $R_0(2/3)$ was calculated to be 45 Å.

The energy-transfer efficiency was determined by donor quenching and sensitized acceptor emission. Donor quenching was monitored at 440 nm (λ_{ex} = 390 nm), and sensitized emission was monitored at 520 nm (λ_{ex} = 390 nm). The emission intensities F^D_D and F^D_A were determined from the fluorescence spectra of tRNA^{fMet}(8–13) and tRNA^{fMet}(3′-Flc), respectively. The energy-transfer parameters for tRNA^{fMet}-(8–13,3′-Flc) are summarized in Table III. The transfer efficiency measured by donor quenching and sensitized emission are in agreement.

Since the quantum yield and spectra of the tRNA^{fMet}(8–13) are not changed upon binding of MetRS, any MetRS-induced changes in the 8–13 emission intensity of tRNA^{fMet}(8–13,3′-Flc) reflect a change in the energy-transfer efficiency between the 8–13 donor and the 3′-Flc acceptor. The 3′-Flc excitation wavelength maximum is red-shifted 5 nm, upon the binding of tRNA^{fMet}(8–13,3′-Flc) to MetRS. The slight shift in the 3′-Flc excitation spectrum reduces the overlap integral, but did not result in significant change in $R_0(2/3)$. tRNA^{fMet}(8–13,3′-Flc) was titrated with MetRS, and the 8–13

Table III: Energy-Transfer Parameters for Free and MetRS-Bound $tRNA^{fMet}$(8–13,3′-Flc)

parameter[a]	free $tRNA^{fMet}$(8–13,3′-Flc)	MetRS-bound $tRNA^{fMet}$-(8–13,3′-Flc)
donor	8–13	8–13
acceptor	3′-Flc	3′-Flc
J (M^{-1} cm^{-1} nm^4)	9.7×10^{14}	9.2×10^{14}
ϕ_D	0.60	0.60
$R_0(2/3)$ (Å)	45	45
E_D	0.51	0.48
E_A	0.52	nd
f_A (mol of acceptor/mol of $tRNA^{fMet}$)	0.98	0.98
E_D^{cor}	0.52	0.49
$R(2/3)$ (Å)	44	45
$R(2/3)/R$	0.89–1.10	0.88–1.13
R (Å)	40–50	40–51

[a] The parameters are defined under Materials and Methods and in Table II.

Table IV: Energy-Transfer Parameters for Free and MetRS-Bound $tRNA^{fMet}$(3′-Flc,D-Etd)

parameter[a]	free $tRNA^{fMet}$-(3′-Flc,D-Etd)	MetRS-bound $tRNA^{fMet}$(3′-Flc,D-Etd)
donor	3′-Flc	3′-Flc
acceptor	D-Etd	D-Etd
J (M^{-1} cm^{-1} nm^4)	3.0×10^{14}	3.0×10^{14}
ϕ_D	0.84	0.50
$R_0(2/3)$ (Å)	40	37
E_D	0.17	0.07
E_A	0.15	nd
f_A (mol of acceptor/mol of $tRNA^{fMet}$)	0.75	0.75
E_D^{cor}	0.23	0.09
$R(2/3)$ (Å)	49	54
$R(2/3)/R$	0.91–1.08	0.91–1.11
R (Å)	45–54	49–59

[a] The parameters are defined under Materials and Methods and in Table II.

emission intensity was monitored. The change in $1 - E_D$ with MetRS is shown in Figure 2. Upon binding of $tRNA^{fMet}$(8–13,3′-Flc) to MetRS, the 8–13 emission intensity is increased by 6%. The increase in 8–13 emission intensity corresponds to a decrease in the transfer efficiency from 0.52 in free tRNA to 0.49 in MetRS-bound tRNA (Table III).

The apparent distances between the 8–13 and the 3′-Flc fluorophores in free and MetRS-bound $tRNA^{fMet}$(8–13,3′-Flc) are determined to be 40–50 and 40–51 Å, respectively. The observed decrease in the transfer efficiency, upon the binding of $tRNA^{fMet}$(8–13,3′-Flc) to MetRS, may result from a change in the average relative orientation or distance between the 8–13 and the 3′-Flc fluorophores.

$tRNA^{fMet}$(3′-Flc,D-Etd). $tRNA^{fMet}$(3′-Flc,D-Etd) was prepared, and the labeling stoichiometry was determined to be 0.75 mol of D-Etd and 0.92 mol of Flc per mole of $tRNA^{fMet}$.

The absorption, excitation, and emission maximum wavelengths, emission anisotropy, and Perrin plot's limiting anisotropy and slope of the 3′-Flc fluorophore in $tRNA^{fMet}$(3′-Flc,D-Etd) are identical with those in $tRNA^{fMet}$(3′-Flc) (Table I). The fluorescence properties of the D-Etd in $tRNA^{fMet}$-(3′-Flc,D-Etd) could not be determined directly because of the large contribution of 3′-Flc emission, and therefore, these properties were not compared with those for single-labeled $tRNA^{fMet}$(D-Etd). The energy-transfer parameters for $tRNA^{fMet}$(3′-Flc,D-Etd) are summarized in Table IV. The

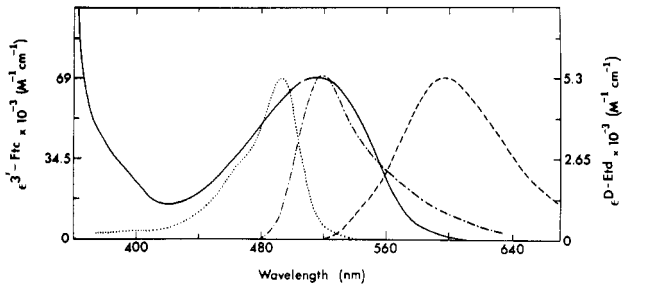

FIGURE 4: Spectral relationships characterizing the 3′-Flc donor and the D-Etd acceptor in $tRNA^{fMet}$(3′-Flc,D-Etd). The absorption (···) and corrected emission (–·–) spectra for 3′-Flc in $tRNA^{fMet}$(3′-Flc) are shown. Also shown are the absorption (—) and emission (– –) spectra for D-Etd in $tRNA^{fMet}$(D-Etd).

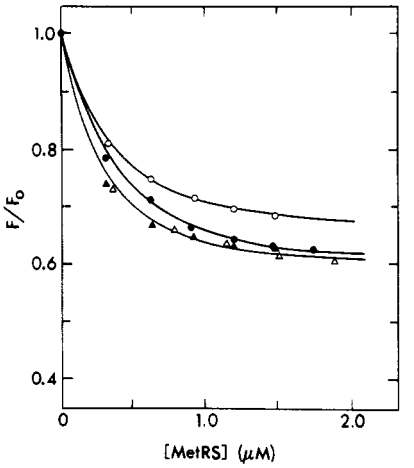

FIGURE 5: Fluorescence titration of 0.31 (▲), 0.37 (△), and 0.44 μM (●) $tRNA^{fMet}$(3′-Flc) with MetRS and the fluorescence titration of 0.41 μM $tRNA^{fMet}$(3′-Flc,D-Etd) (○) with MetRS. The emission intensity of fluorescein was monitored at 520 nm (λ_{ex} = 480 nm). The solid curves fitting the data were calculated with eq 2 in Ferguson & Yang (1986a). The binding parameters of the calculated curves fitting the data for $tRNA^{fMet}$(3′-Flc) are K = 0.13 μM, $(F/F_0)_{max}$ = 0.59, and n = 1.0. The binding parameters for the curve fitting the data for $tRNA^{fMet}$(3′-Flc,D-Etd) are K = 0.15 μM, $(F/F_0)_{max}$ = 0.65, and n = 1.0. The uncertainty in $(F/F_0)_{max}$ was estimated to be <±2%.

overlap integral for the 3′-Flc donor and D-Etd acceptor was calculated with the corrected emission spectrum of $tRNA^{fMet}$(3′-Flc) and the absorption spectrum for $tRNA^{fMet}$(D-Etd) (Figure 4). $R_0(2/3)$ was calculated to be 40 Å for the 3′-Flc donor and D-Etd acceptor. Donor quenching, F_{DA}^{D}, was monitored at 520 nm (λ_{ex} = 480 nm), and sensitized emission, F_{DA}^{A}, was monitored at 600 nm (λ_{ex} = 492 nm). The emission intensities of the donor, F_D^D, and the acceptor, F_A^D, were determined from the spectra of $tRNA^{fMet}$(3′-Flc) and $tRNA^{fMet}$(D-Etd), respectively. The transfer efficiency measured by donor quenching (0.17) is in agreement with the transfer efficiency (0.15) measured by sensitized emission (Table IV). The corrected transfer efficiency (0.25) in $tRNA^{fMet}$(3′-Flc,D-Etd) corresponds to an apparent distance 45–54 Å between the 3′-Flc and the D-Etd fluorophores.

The titration of $tRNA^{fMet}$(3′-Flc) and $tRNA^{fMet}$(3′-Flc,D-Etd) with MetRS, as monitored by the fluorescein fluorescence at 520 nm (λ_{ex} = 480 nm), is shown in Figure 5. The two 3′-Flc-labeled $tRNA^{fMet}$s bind to MetRS with slightly different binding affinity. A portion of the reduced extent of quenching of 3′-Flc emission, upon the binding of $tRNA^{fMet}$(3′-Flc,D-Etd) to MetRS, results from a slight decrease in the affinity of double-labeled $tRNA^{fMet}$ toward MetRS. After corrections for these differences, as shown in Figure 2, the transfer ef-

ficiency between the 3′-Flc donor and the D-Etd acceptor decreases with increasing MetRS concentration. The transfer efficiency decreased from 0.23 to 0.09, upon the complete binding of tRNA^{fMet}(3′-Flc,D-Etd) to MetRS. The characteristic distance, $R_0(2/3)$, for the 3′-Flc donor and the D-Etd acceptor is decreased when tRNA^{fMet}(3′-Flc,D-Etd) is complexed with MetRS, from 40 to 37 Å, due to the MetRS-induced decrease in 3′-Flc quantum yield. The energy-transfer measurement for MetRS-bound tRNA^{fMet}(3′-Flc,D-Etd) corresponds to an apparent distance between the 3′-Flc and the D-Etd fluorophores of 49–59 Å.

Discussion

In the present investigation, the conformations of tRNA^{fMet} and MetRS-bound tRNA^{fMet} are analyzed with tRNA^{fMet} labeled with two fluorophores. Three species of tRNA^{fMet} modified at two of the three sites including the 3′-end, dihydrouridine, and 8–13 were used. The binding affinity for each of the modified forms of tRNA^{fMet} to MetRS was slightly reduced but comparable to that of the unmodified tRNA^{fMet}. Each of the double-labeled tRNA^{fMet} was found to induce close to the same extent of MetRS tryptophan quenching as unmodified tRNA^{fMet}. These results suggest that the interaction of the labeled tRNA^{fMet} with MetRS is very similar to that of unmodified tRNA^{fMet}. The conclusions drawn from the present studies may be reasonably extended to the interaction between unmodified tRNA^{fMet} and MetRS.

The quantitative relationship between the transfer efficiency and the distance separating the donor and the acceptor has long been established (Forster, 1966; Cantor & Schimmel, 1980). Besides the relative proximity, the transfer efficiency is apparently affected by the spectral overlap, orientation, sizes, shapes, rotational freedom, and spatial distribution of the emission and absorption dipoles of the donor and the acceptor groups. In practice, an apparent distance is calculated by assuming random orientation ($K^2 = 2/3$). In addition, a range of apparent distances is obtained on the basis of the fluorescence polarization of the donor and the acceptor (Haas et al., 1978; Dale & Eisenger, 1979).

tRNA^{fMet}(8–13,D-Etd) showed reduced but appreciable methionine acceptor activity and MetRS binding affinity (based on the tryptophan quenching) comparable to that of unmodified tRNA^{fMet}. Highly efficient energy transfer between 8–13 and D-Etd was observed by donor quenching and sensitized emission. The transfer efficiency was not changed in the presence of MetRS, suggesting that any conformational changes at 8–13 or D20 are not sufficient to reduce or enhance the transfer efficiency.

The 3′-terminus in tRNA^{fMet} has been shown previously to be highly flexible in free tRNA and to be rigid in MetRS-bound tRNA^{fMet} (Ferguson & Yang, 1986a). As a result, the apparent distance between the 3′-terminus and 8–13 or D20 is the weighted average of the actual distances of all possible 3′-terminal conformations. The 3′-terminal unpaired nucleotides showed an extended conformation continuing the helix of the amino acid acceptor stem in tRNA^{Phe} (Kim et al., 1974; Robertus et al., 1974) and showed a conformation folded back toward the amino acid acceptor stem in tRNA^{fMet} (Woo et al., 1980). These crystal structures may be representative of two of the possible 3′-terminal conformations in equilibrium in solution. Additional 3′-terminal flexibility may be mediated through the covalent linkage between the 3′-terminal adenosine and the fluorophore. Since the transfer efficiency is inversely proportional to the sixth power of the distance, the results of energy-transfer experiments in these cases weigh heavily toward those conformations with short distances.

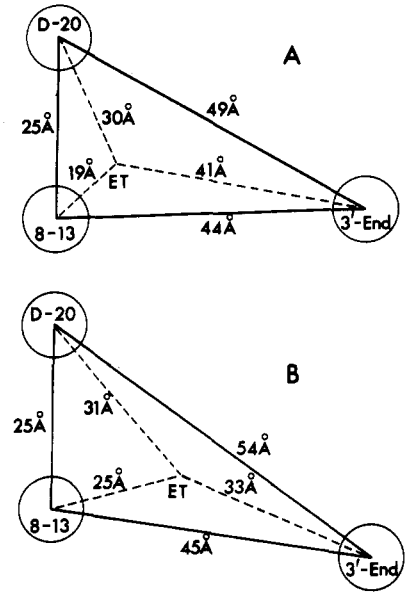

FIGURE 6: Relative proximity of the 3′-end; D20, 8–13, and the ethidium binding site in free tRNA^{fMet} (A) and methionyl-tRNA synthetase bound tRNA^{fMet} (B). Distances are drawn in proportion to the apparent distances except those including the ethidium binding site (Ferguson & Yang, 1986c), which is located out of the plane of the 3′-end, D20, and 8–13. The actual distances are most probably within the 4-Å spheres surrounding the sites.

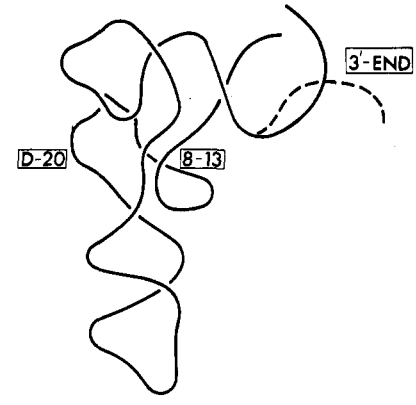

FIGURE 7: Conformation of tRNA^{fMet} in comparison with the plausible 3′-terminal conformation in the tRNA^{fMet}–MetRS complex (dashed line).

Upon binding of MetRS, the 3′-terminus has been shown to be rigidly bound in a nonpolar environment in MetRS (Ferguson & Yang, 1986a). The apparent distance between 3′-terminus and 8–13 is slightly increased, and that between the 3′-terminus and D20 is appreciably increased (from 49 to 54 Å).

The relative locations of the 3′-terminus, D20, and 8–13 in free and MetRS-bound tRNA^{fMet} are shown schematically in Figure 6 (together with the apparent distances to the ethidium binding site previously determined by energy-transfer experiments; Ferguson & Yang, 1986c). The shift at the 3′-terminus is apparent and is close to 5 Å. Since the synthetase is most likely binding the inner loop of the L-shaped tRNA (Rich & Schimmel, 1977), the 5-Å shift of the 3′-terminus away from D20 suggests that the 3′-terminus is moving toward the synthetase upon binding of MetRS. One such conformation is illustrated in Figure 7. The main feature of the MetRS-bound conformation is the bending of the 3′-terminal strand as compared to the crystal structure of free tRNA^{Phe} (Table V). Such a conformation is consistent with the results of neutron scattering studies of the tRNA^{fMet}–MetRS complex

Table V: MetRS-Induced Conformational Changes in $tRNA^{fMet}$

locations	distances (Å)		
	-MetRS	+MetRS	crystallography[b]
8–13 to 3′-end	44	45	50
8–13 to D20	25	25	17
3′-end to D20	49	54	60

[a] The orientation factor, K^2, is assumed to be 2/3. [b] Measurements using yeast $tRNA^{Phe}$ and the computer display program developed by Dr. B. K. Lee.

(Dessen et al., 1982), which suggest considerable flexibility must be imposed on $tRNA^{fMet}$ upon complex formation, such that the 3′-end can bind close to the center of the enzyme (Zelwer et al., 1980) and still allow the centers of mass of the enzyme and of tRNA to overlap.

Bending of the 3′-terminal single-stranded region of $tRNA^{fMet}$ toward synthetase may be a general characteristic in tRNA–synthetase complex formation and possibly other RNA–protein interactions. The flexibility at the 3′-terminus and its bending in the tRNA–synthetase complex may be important in the kinetics of the tRNA–synthetase interaction. A flexible target site in a macromolecule can significantly increase the corresponding target area during the recombination of the interacting macromolecules, and hence enhance the second-order rate constant.

3′-Terminal nucleotides in tRNA evidently play an essential role in the tRNA–synthetase interaction (von der Haar & Gaertner, 1975; Krauss et al., 1977). We have previously observed delocalized conformational changes in $tRNA^{fMet}$ upon binding of MetRS (Ferguson & Yang, 1986a) and unsymmetric conformational changes in the two subunits in MetRS upon binding of $tRNA^{fMet}$ (Ferguson & Yang, 1986b). It is necessary to determine the structural and kinetic relationship of these conformational changes with the bending of the 3′-terminal strand in order to further elucidate the recognition process. Preliminary results suggest that the 3′-terminus has a pivotal role in the conformational changes in MetRS (B. Q. Ferguson and D. C. H. Yang, unpublished results). It is likely that MetRS in the newly formed conformation after binding the 3′-terminus subsequently interacts with the bulk of the tRNA molecule to form the final stable tRNA–synthetase complex.

In summary, the intramolecular distance measurements suggest little changes in the overall conformation of tRNA except at the 3′-terminus. The results suggest that the 3′-terminal arm in the amino acid acceptor stem in $tRNA^{fMet}$ bends toward the inner loop of the L-shaped tRNA upon binding of MetRS, in contrast to the continuing helix shown in the crystal structure of free tRNA. It appears that tRNA–synthetase complex formation involves the immobilization, shielding (Ferguson & Yang, 1986a), and bending of the 3′-terminal strand in the amino acid acceptor stem of $tRNA^{fMet}$.

ACKNOWLEDGMENTS

We gratefully acknowledge discussions with Dr. B. K. Lee (NIH) and the use of the display program in the analysis of the crystallographic data of $tRNA^{Phe}$.

Registry No. Flc, 2321-07-5; Etd, 3546-21-2.

REFERENCES

Ackerman, E. J., Joachimiak, A., Klinghofer, V., & Sigler, P. (1985) *J. Mol. Biol. 181*, 93–102.

Beardsley, K., & Cantor, C. R. (1970) *Proc. Natl. Acad. Sci. U.S.A. 65*, 39–46.

Cantor, C. R., & Schimmel, P. R. (1980) in *Biophysical Chemistry*, Freeman, New York.

Cassio, D., & Waller, J. P. (1974) *Eur. J. Biochem. 20*, 283–300.

Dale, R. E., & Eisinger, J. (1979) *Biophys. J. 26*, 161–194.

Dessen, P., Fayat, G., Zaccai, G., & Blanquet, S. (1982) *J. Mol. Biol. 154*, 603.

Engel, G. (1974) *Anal. Biochem. 61*, 184–191.

Fairclough, R. H., & Cantor, C. R. (1978) *Methods Enzymol. 48*, 347–379.

Fairclough, R. H., & Cantor, C. R. (1979) *J. Mol. Biol. 132*, 575–586.

Favre, A., Mechelson, A. M., & Yaniv, M. (1971) *J. Mol. Biol. 58*, 367–379.

Ferguson, B. Q., & Yang, D. C. H. (1986a) *Biochemistry 25*, 529–539.

Ferguson, B. Q., & Yang, D. C. H. (1986b) *Biochemistry 25*, 2743–2748.

Ferguson, B. Q., & Yang, D. C. H. (1986c) *Biochemistry* (in press).

Forster, T. (1966) in *Modern Quantum Chemistry* (Sinanoglu, O., Ed.) Section III, pp 93–137, Academic, New York.

Haas, E., Katzir, E. K., & Steinberg, I. Z. (1978) *Biochemistry 17*, 5064–5070.

Holler, E., Baltzinger, M., & Favre, A. (1981) *Biochemistry 20*, 1139–1147.

Hountondji, C., Blanquet, S., & Lederer, F. (1985) *Biochemistry 24*, 1175–1180.

Kim, S. H., Suddath, F. L., Quigley, G. J., McPherson, A., Sussman, J. C., Wang, A., Seeman, N. C., & Rich, A. (1974) *Science (Washington, D.C.) 185*, 435–440.

Krauss, G., Riesner, D., & Maas, G. (1976) *Eur. J. Biochem. 68*, 81–93.

Rich, A., & Schimmel, P. R. (1977) *Nucleic Acids Res. 4*, 1649–1665.

Robertus, J. D., Ladner, J. E., Finch, J. T., Rhodes, D., Brown, R. S., Clark, B. F. C., & Klug, A. (1974) *Nature (London) 250*, 546–551.

Rosa, J. J., Rosa, M. D., & Sigler, P. B. (1979) *Biochemistry 18*, 637–647.

Schimmel, P. R., & Soll, D. G. (1979) *Annu. Rev. Biochem. 48*, 601–648.

Schulman, L. H., Pelka, H., & Susaui, M. (1983) *Nucleic Acids Res. 11*, 1439–1455.

Shinitzky, M. (1972) *J. Chem. Phys. 56*, 5979–5981.

Uemura, H., Imai, M., Ohtsuka, E., Ikahara, M., & Soll, D. (1982) *Nucleic Acids Res. 10*, 6531–6539.

von der Haar, F., & Gaertner, E. (1975) *Proc. Natl. Acad. Sci. U.S.A. 72*, 1378–1382.

Wells, B. D., & Cantor, C. R. (1977) *Nucleic Acids Res. 4*, 1668–1680.

Wells, B. D., & Cantor, C. R. (1980) *Nucleic Acids Res. 8*, 3229–3246.

Wetzel, R., & Soll, D. (1977) *Nucleic Acids Res. 4*, 1681–1694.

Wintermeyer, W., & Zachau, H. G. (1979) *Eur. J. Biochem. 98*, 465–475.

Woo, N. H., Roe, B. A., & Rich, A. (1980) *Nature (London) 286*, 346–351.

Wrede, P., Woo, N. H., & Rich, A. (1979) *Proc. Natl. Acad. Sci. U.S.A. 76*, 3289–3293.

Yang, C. H., & Soll, D. G. (1974) *Proc. Natl. Acad. Sci. U.S.A. 71*, 2838–2842.

Zelwer, C., Risler, J. L., & Brunie, S. (1982) *J. Mol. Biol. 155*, 63–81.